Current Biology, Vol. 13, 1549–1556, September 2, 2003, ©2003 Elsevier Science Ltd. All rights reserved. DOI 10.1016/S0960-9822(03)00542-6

DNA Damage Foci at Dysfunctional Telomeres

Hiroyuki Takai, Agata Smogorzewska, and Titia de Lange*
Laboratory for Cell Biology and Genetics
The Rockefeller University
New York, New York 10021

Summary

We report cytologic and genetic data indicating that telomere dysfunction induces a DNA damage response in mammalian cells. Dysfunctional, uncapped telomeres, created through inhibition of TRF2, became associated with DNA damage response factors, such as 53BP1, γ-H2AX, Rad17, ATM, and Mre11. We refer to the domain of telomere-associated DNA damage factors as a Telomere Dysfunction-Induced Focus (TIF). The accumulation of 53BP1 on uncapped telomeres was reduced in the presence of the PI3 kinase inhibitors caffeine and wortmannin, which affect ATM, ATR, and DNA-PK. By contrast, Mre11 TIFs were resistant to caffeine, consistent with previous findings on the Mre11 response to ionizing radiation. A-T cells had a diminished 53BP1 TIF response, indicating that the ATM kinase is a major transducer of this pathway. However, in the absence of ATM, TRF2 inhibition still induced TIFs and senescence, pointing to a second ATM-independent pathway. We conclude that the cellular response to telomere dysfunction is governed by proteins that also control the DNA damage response. TIFs represent a new tool for evaluating telomere status in normal and malignant cells suspected of harboring dysfunctional telomeres. Furthermore, induction of TIFs through TRF2 inhibition provides an opportunity to study the DNA damage response within the context of well-defined, physically marked lesions.

Results and Discussion

Telomere dysfunction has been implicated in tumorigenesis and aging (reviewed in [1–4]), yet little is known about the mechanisms by which mammalian cells perceive and respond to the loss of telomere function. Telomere uncapping occurs when cells have critically shortened telomeres or when telomere-protective factors are impaired (reviewed in [5]). Under either circumstance, loss of telomere function can induce cell cycle arrest, senescence, apoptosis, and chromosome end fusions, outcomes that are consistent with the activation of a DNA damage response. Supporting the view that telomere uncapping leads to a DNA damage response, loss of telomere protection by TRF2 results in ATM- and p53-dependent apoptosis, [6] and telomere shortening activates p53 in a variety of human and mouse cell types [7–9]. While suggestive, none of these findings provide direct evidence that dysfunctional telomeres are recognized by the DNA damage machinery. Here, we show that experimentally uncapped telomeres invoke the earliest known cellular response to DNA damage, the formation of foci containing DNA damage response factors.

In this study, telomere uncapping is achieved through inactivation of the duplex TTAGGG repeat binding factor TRF2 [5, 10, 11], which is essential for telomere protection. TRF2 is inhibited by using RNAi or a dominant-negative TRF2 allele ($TRF2^{\Delta B\Delta M}$), which prevents accumulation of the endogenous TRF2 on telomeres [12]. Although the duplex telomeric DNA remains intact when TRF2 is inhibited, much of the single-stranded 3′ overhang disappears and telomeres undergo nonhomologous end joining [12, 13]. $TRF2^{\Delta B\Delta M}$ induces apoptosis in lymphocytes [6] and senescence in primary fibroblasts [14].

If uncapped telomeres resemble damaged DNA, they might become associated with DNA damage response factors, such as 53BP1, Mre11, and phosphorylated forms of Rad17, H2AX, and ATM [15–20]. To test this, hTERT-immortalized BJ human fibroblasts were infected with a $TRF2^{\Delta B\Delta M}$ adenovirus [6]. As a control, cells were infected in parallel with a β-galactosidase virus. Within 2 days of infection, the expression of $TRF2^{\Delta B\Delta M}$ induced numerous 53BP1 foci, and dual staining indicated that many of the foci colocalized with TRF1 and therefore represented telomeric loci (Figures 1A and 1B). Scoring of 75 nuclei showed a mean of 11.0 (SD = 11.1; range 0–39) 53BP1 foci per nucleus (examining one focal plane per nucleus), and of these, 60% colocalized with TRF1. In contrast, 53BP1 foci induced by IR did not colocalize with TRF1 (Figure 1A). Although the mean number of IR-induced 53BP1 foci was 30 per cell (SD = 7.6, n = 25), only 1 or 2 of these foci colocalized with TRF1. Thus, the localization of 53BP1 to telomeres was specifically induced by inhibition of TRF2.

Images obtained by using a deconvolution microscope further confirmed the colocalization of 53BP1 with TRF1 and showed that the 53BP1 domain often extended considerably beyond the region of TRF1 staining (Figure 1B). This suggested that a large subtelomeric region became associated with 53BP1. The same effect was observed when the fluorophores were switched (TRF1 detected with FITC and 53BP1 detected with TRITC; data not shown). Therefore, we conclude that the 53BP1 domain is larger than the telomeric chromatin domain, as defined by the presence of TRF1.

We refer to the 53BP1 foci at uncapped telomeres as Telomere Dysfunction-Induced Foci, or TIFs. TIFs are defined as foci of DNA damage response factors that coincide with TRF1 signals. Although other DNA damage response factors also localize to telomeres (see below), TIFs are most easily detected with 53BP1 antibodies. We quantified the TIF response by examining the colocalization of 53BP1 and TRF1 in 25 nuclei (single focal plane for each nucleus). Cells were considered TIF positive if they contained four or more 53BP1 foci that colocalized with TRF1. Most of the TIF-positive cells contained more than four 53BP1 foci at telomeres (mean 12.6, SD = 7.4, n = 38). While the fraction of TIF-positive

*Correspondence: delange@mail.rockefeller.edu

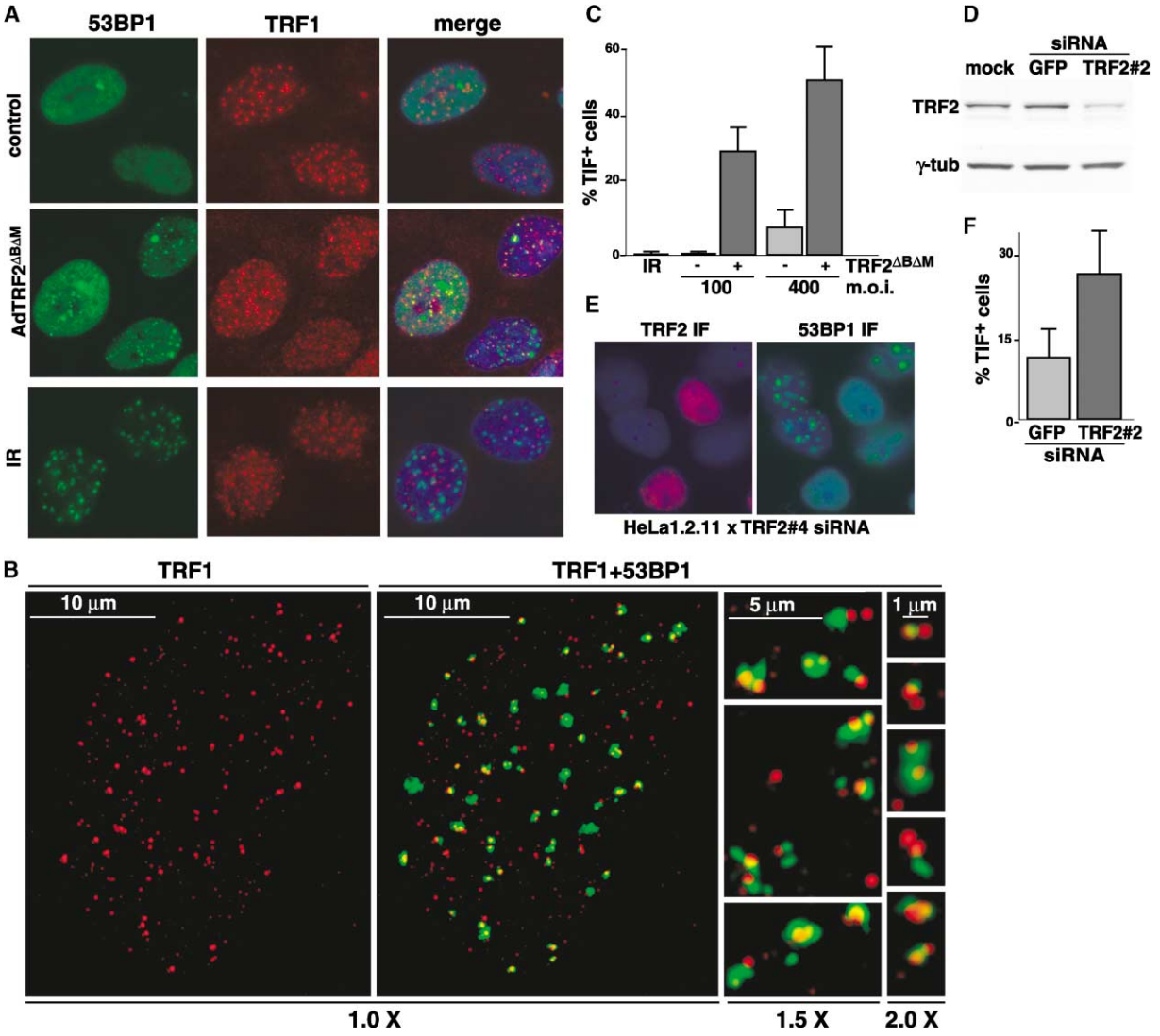

Figure 1. Binding of 53BP1 to Uncapped Telomeres

(A) TRF2$^{\Delta B \Delta M}$, but not IR, induced telomeric localization of 53BP1. hTERT-BJ cells were infected with the indicated adenoviruses (control: β-galactosidase virus), were fixed 48–52 hr postinfection, and were processed for 53BP1 (green) and TRF1 (red) IF. DNA was stained (DAPI, blue) in the merged images. IR: 2 Gy treatment, followed by IF after 1 hr.

(B) DeltaVision images. Infection and IF are as described in (A). The left images show a single nucleus. The enlarged images show additional 53BP1 foci at telomeres from this and other nuclei.

(C) TIF index (percentage of TIF-positive cells) of TRF2$^{\Delta B \Delta M}$-expressing (+) and vector control (−) hTERT-BJ cells. Cells with four or more 53BP1 foci colocalizing with TRF1 were scored as TIF positive (n = 75; SDs from three independent experiments). The multiplicity of infection (m.o.i.) is as indicated.

(D) An immunoblot of a TRF2 knockdown with TRF2 siRNA. Whole-cell lysates of HeLaII cells harvested 48 hr after siRNA transfection with the indicated siRNAs.

(E) HeLa1.2.11 cells transfected with TRF2 siRNA (#4), processed 72 after the first transfection for TRF2 or 53BP1 IF.

(F) Induction of TIFs with TRF2 siRNA. HeLaII cells were fixed and processed for 53BP1 and TRF1 IF 48 hr after the first transfection of siRNA (TRF2 siRNA #2). The TIF index (n = 25, from one experiment) is as in (C).

cells is negligible in control cultures, 30%–60% of the cells infected with the TRF2$^{\Delta B \Delta M}$ adenovirus were TIF positive (Figure 1C and see below).

Induction of 53BP1 foci at telomeres was also observed after TRF2 inhibition with RNAi in HeLa cells (Figures 1D and 1E). Some HeLa subclones have a considerable basal level of 53BP1 foci in the absence of TRF2 inhibition (data not shown); this same phenomenon has been described for several other tumor cell lines [21]. However, these foci rarely colocalize with TRF1 and do not affect the outcome of the TRF2 siRNA experiments. Two independent TRF2 siRNAs (#2 and #4) reduced the expression of TRF2 considerably, as detected by Western blotting and IF with two different HeLa cell lines (Figures 1D and 1E). Cells with reduced TRF2 levels developed 53BP1 foci (Figure 1E) and showed a significant increase in the fraction of TIF-positive cells as compared to cells treated with a control siRNA to GFP (Figure

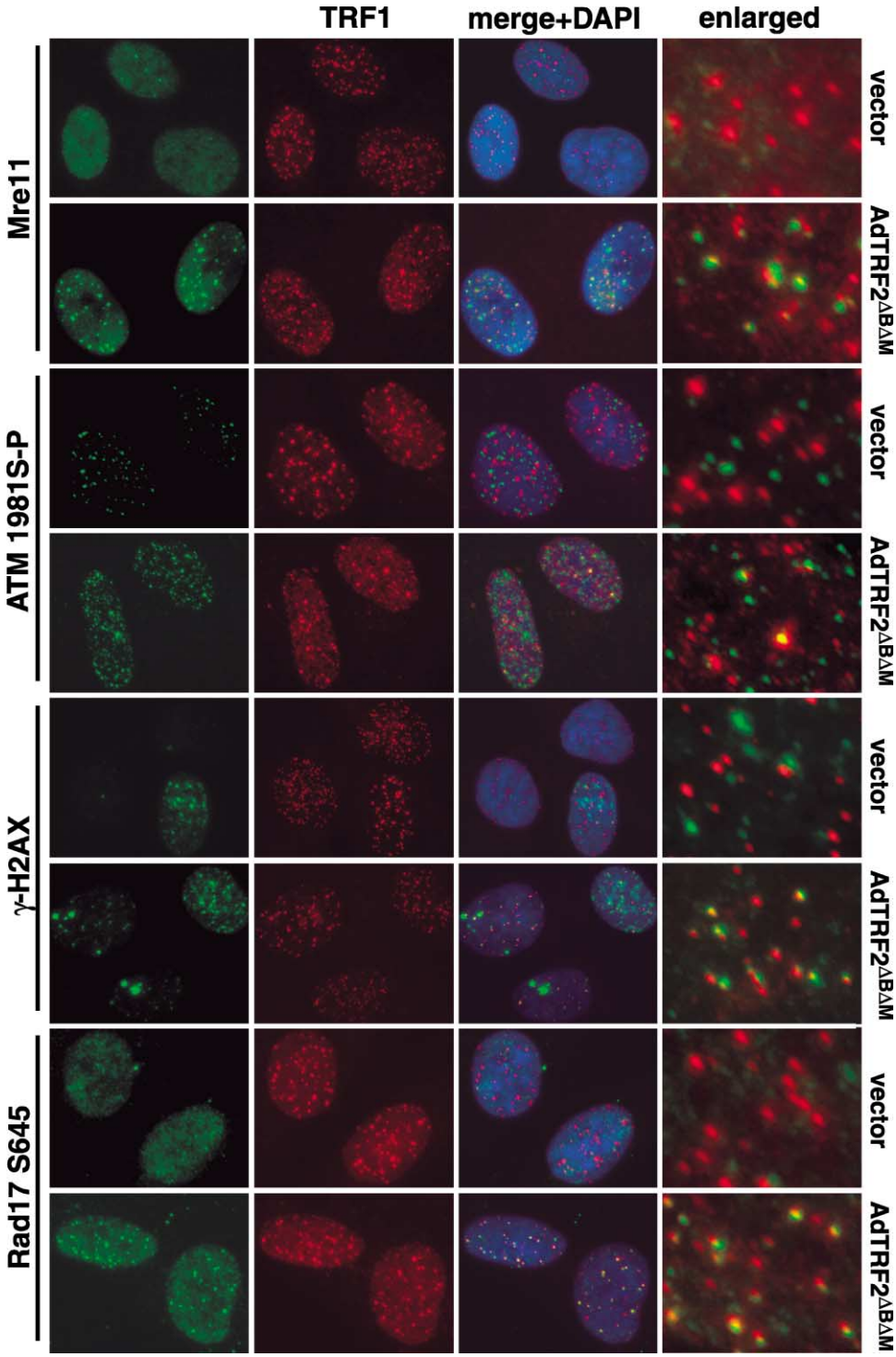

Figure 2. Accumulation of Mre11 and Phosphorylated ATM, H2AX, and Rad17 on Uncapped Telomeres

hTERT-BJ cells were infected as in Figure 1A and were processed for IF by using antibodies to TRF1 (red) and Mre11, Ser 1981-phosphorylated ATM, γ-H2AX, or Ser 645-phosphorylated Rad17 (green). Enlarged views of the merged images are shown to the right. DNA was stained by DAPI (blue).

1F). These data corroborate the idea that the binding of DNA damage response factors to telomeres in cells expressing the dominant-negative allele of TRF2 is due to diminished TRF2 function.

In addition to 53BP1, TIFs contained other well-established DNA damage response factors, such as the Mre11 complex, ATM, H2AX, and Rad17 (Figure 2) [15–19]. In control cells, the Mre11 complex showed the previously

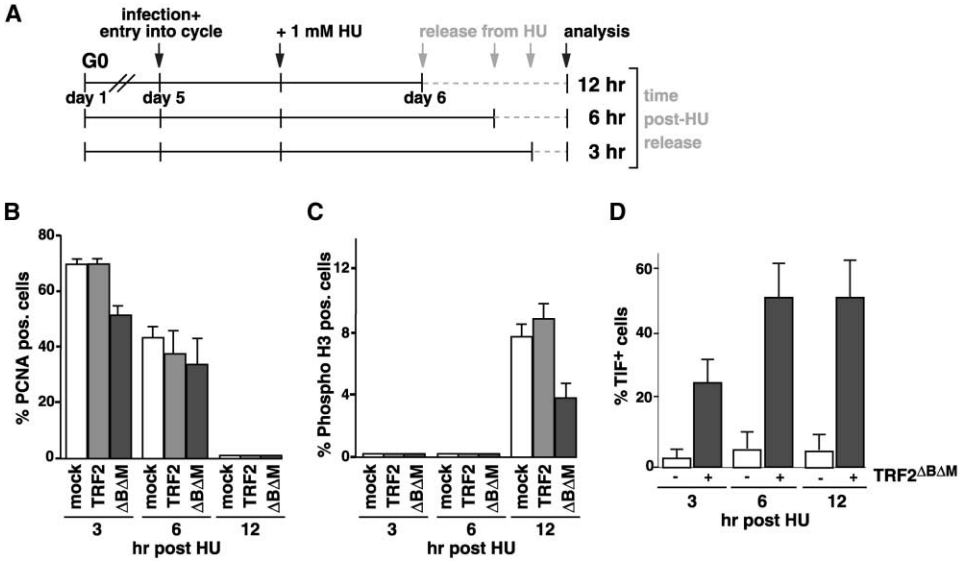

Figure 3. Progression through Mitosis Is Not Required for TIF Formation

(A) The experimental time line. Contact-inhibited hTERT-BJ cells were infected with adenovirus (100 pfu/cell) and were replated at low density. Media containing 1 mM HU was added after 12 hr, resulting in G1/S arrest. Cells were fixed and processed for TIF analysis or stained with S phase (PCNA) or M phase (Ser 10-phosphorylated histone H3) markers at 3, 6, and 12 hr after release from HU.

(B) S phase index at the indicated time points as determined by PCNA staining in mock-infected cells, TRF2 (full length)-infected cells, and cells infected with $TRF2^{\Delta B\Delta M}$ (indicated by ΔBΔM).

(C) The mitotic index at the indicated time points as determined by staining for phospho H3. Cell populations and time points are as in (B).

(D) The TIF index of cells infected with full-length TRF2 virus (−) or $TRF2^{\Delta B\Delta M}$ virus (+) at the indicated time points after release from HU.

noted IF pattern with most of the signal localizing to PML bodies [17]. A small amount of Mre11 has been shown to localize at telomeres [22], but this fraction is not detectable under the conditions used here. After introduction of $TRF2^{\Delta B\Delta M}$, many of the cells showed prominent Mre11 signals at telomeric sites (Figure 2). Furthermore, phosphorylated histone H2AX (γ-H2AX), activated ATM phosphorylated on Ser 1981, and Rad17 phosphorylated on Ser 645 formed foci at telomeres after inhibition of TRF2 (Figure 2). As was noted for 53BP1, the Mre11, ATM, γ-H2AX, and Rad17 domains often extended beyond the area of TRF1 staining. These findings confirm and extend the previous inference that γ-H2AX occupies a very large region surrounding the site of damage [23]. $TRF2^{\Delta B\Delta M}$-mediated telomere uncapping is known to leave the double-stranded telomeric DNA intact and results in a reduction of the TTAGGG repeat overhang that normally protrudes 50–200 nt 3′ [12]. We infer from this knowledge that the binding of Mre11, ATM, H2AX, 53BP1 and Rad17 to uncapped telomeres takes place at sites that do not contain extensive regions of single-stranded DNA.

Using synchronized cultures, we found that cells became TIF positive in the first S phase or G2 phase after infection with the $TRF2^{\Delta B\Delta M}$ adenovirus (Figure 3). This indicated that progression through mitosis is not required for the TIF response. TIF-positive cells were rare before the onset of DNA replication (data not shown) and were primarily observed after cells had begun S phase (Figures 3B–3D). These findings suggest that DNA replication promotes TIF formation. Consistent with this, many of the telomeres in TIF-positive cells appeared as double dots, indicating that they have been duplicated (for instance, see Figure 1B). Therefore, TIF-positive cells are most likely to occur in late S phase or in G2 phase. In some cases, both sister telomeres are associated with 53BP1 (see enlarged inserts; Figure 1B). However, in other cases, only one of the two sister telomeres contained detectable 53BP1, suggesting that telomere uncapping occurred during or after DNA replication. Perhaps DNA replication contributes to the formation or sensing of the uncapped state at telomeres. It is also possible that the inhibition of TRF2 with the dominant-negative allele is enhanced during S phase.

We determined whether the TIF response depended on signal transduction by PI3 kinases, such as ATM and ATR [24]. Treating cells with the PI3 kinase inhibitors caffeine and wortmannin resulted in a significant reduction in the accumulation of 53BP1 at telomeres in $TRF2^{\Delta B\Delta M}$-infected cells (Figures 4A and 4B). Caffeine consistently reduced the percentage of TIF-positive cells by 3- to 5-fold (Figure 4B). Interestingly, the TIFs were strongly reduced even after 1 hr of caffeine treatment. The most likely explanation is that TIFs require ongoing signaling for their persistence. In contrast to the effect of caffeine on 53BP1, the binding of the Mre11 complex to telomeric sites was not affected by caffeine (Figure 4C). This finding is consistent with a previous report documenting the formation of DNA damage response foci by the Mre11 complex in the presence of caffeine [25]. The caffeine-resistant binding of the Mre11 complex to uncapped telomeres further bolsters the view that this complex can act as a sensor of DNA damage [18] and corroborates the idea that uncapped telomeres resemble DNA lesions.

In order to address the role of the ATM kinase in the

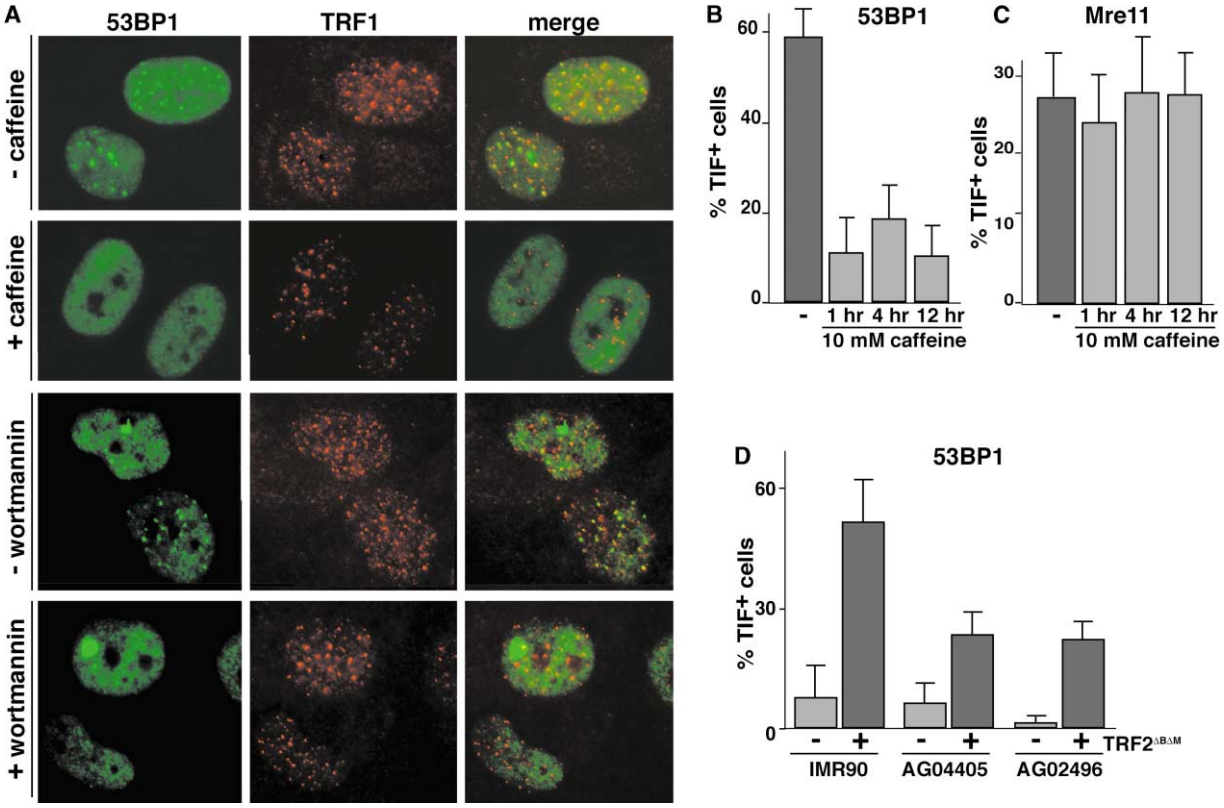

Figure 4. Telomeric Binding of 53BP1, but Not Mre11, Is Affected by PI3-Kinase Inhibitors and ATM Status

(A) Inhibition of 53BP1 TIF formation by caffeine and wortmannin. TRF2$^{\Delta B \Delta M}$-expressing hTERT-BJ cells were treated with 10 mM caffeine or 50 μM wortmannin for 4 hr before fixation.

(B) The TIF index determined by using 53BP1 of hTERT-BJ cells treated with caffeine as in (A) at the indicated time points.

(C) The TIF index determined by using Mre11 of hTERT-BJ cells treated with caffeine as in (A) at the indicated time points.

(D) Reduced induction of TIFs in ATM-defective A-T fibroblasts. Asynchronously grown A-T fibroblasts (AG04405 and AG02496), or normal human IMR90 fibroblasts, were infected with TRF2$^{\Delta B \Delta M}$-expressing adenovirus or control adenovirus, fixed 48–52 hr after infection, and processed for TIF analysis by 53BP1/TRF1 IF.

binding of 53BP1 to telomeres more directly, we tested whether TRF2 inhibition could induce TIF-positive cells in fibroblasts derived from ataxia telangiectasia (A-T) patients, which are deficient in this kinase (reviewed in [24]). The absence of the ATM kinase was verified by Western blotting (see below). The TIF response in two A-T cell strains was diminished compared to ATM-proficient cells (Figure 4D). These data indicate that the ATM kinase is a main transducer of the telomere damage signal. However, since A-T-deficient cells have a residual level of TIF formation, other signal transducers contribute as well.

At the cellular level, the outcome of TRF2 inhibition is either apoptosis or senescence. The apoptotic response is attenuated in A-T cells [6], and this attenuation is consistent with the ATM kinase being involved in the telomere damage signaling pathway. In order to examine the role of the ATM kinase in the senescence response, TRF2$^{\Delta B \Delta M}$ was introduced by retroviral infection into three ATM-deficient A-T fibroblast strains; an ATM-proficient heterozygous parental cell strain was used as a control (Figure 5A). The cell cycle arrest response to TRF2$^{\Delta B \Delta M}$ was documented by measuring BrdU incorporation in comparison to control cultures infected with the empty retroviral vector [13]. TRF2$^{\Delta B \Delta M}$ induced a growth arrest in all three A-T fibroblast strains, and the extent and kinetics of this arrest was similar to that of A-T heterozygous and wild-type fibroblasts (Figure 5B; [13]). Furthermore, the cells expressed SA-β-galactosidase, acquired a senescent morphology, and had increased levels of p21 and p16 (Figures 5C and 5D). Therefore, we conclude that absence of the ATM kinase is not sufficient to abrogate telomere-directed senescence. This is consistent with the observation that replicative senescence of A-T cells can be bypassed by telomerase [26, 27].

The binding of 53BP1, Mre11, and the phosphorylated forms of ATM, H2AX, and Rad17 to uncapped telomeres indicates that cells perceive unprotected chromosome ends as sites of DNA damage. The fact that TIFs are suppressed by caffeine and wortmannin and are diminished in A-T cells is consistent with an ATM-dependent response to dysfunctional telomeres. However, since A-T cells show a residual level of TIF formation and undergo telomere-directed senescence, ATM-independent pathways can be activated. Additional transducers of the telomere damage signal might be ATR or DNA-PKcs. Activation of ATR kinase is thought to require the

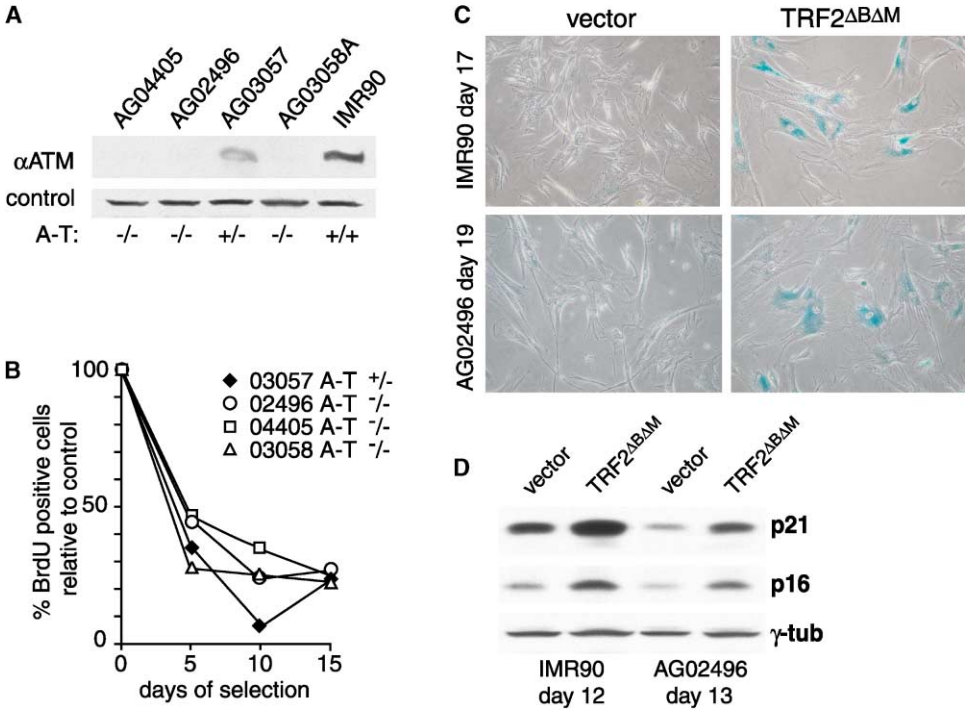

Figure 5. TRF2$^{\Delta B \Delta M}$-Induced Senescence in A-T Fibroblasts

(A) A Western blot confirming the presence or absence of ATM in primary fibroblasts from A-T patients (AG04405, AG02496, AG03058A), the heterozygous mother (AG03057) of one of the affected donors (AG03058A), and normal human primary fibroblasts (IMR90).

(B) Changes in BrdU incorporation in TRF2$^{\Delta B \Delta M}$-expressing A-T cells. S phase cells were identified at the indicated time points based on BrdU incorporation for 5 hr. Changes in BrdU incorporation are represented as the fraction of BrdU-positive cells in TRF2$^{\Delta B \Delta M}$-expressing cells divided by the fraction of BrdU-positive cells in vector control cells. This ratio is set at 100% for day 0.

(C) TRF2$^{\Delta B \Delta M}$ expression induces SA-β-gal activity and senescent morphology in AG02496 A-T cells. Photographs of IMR90 cells and AG02496 cells infected with TRF2$^{\Delta B \Delta M}$-expressing retrovirus or control virus processed for SA-β-gal assay at the indicated time points are shown.

(D) Induction of p21 and p16 by TRF2$^{\Delta B \Delta M}$. An immunoblot with cell lysates from retrovirally infected cells (viruses, time points, proteins, and cells are as indicated).

binding of RPA to single-stranded DNA [28]. As dysfunctional human telomeres do not generate extensive single-stranded regions [12, 29], they may activate ATR relatively poorly. This could explain why ATM is a main telomere signal transducer in human cells, whereas in yeast, where uncapped telomeres are rendered single stranded [30], the ATR ortholog Mec1 plays this role [31].

TIFs are novel markers for telomere dysfunction. Hitherto, the absence of telomere protection could only be deduced from end-to-end chromosome fusions and their associated anaphase bridges. Such assays have limitations since they require progression into mitosis, despite telomere dysfunction. Furthermore, the formation of end-to-end chromosome fusions depends on the removal of the 3′ telomeric overhang and processing of the ends by nonhomologous end joining. In so far as the TIF assay primarily relies on ATM proficiency and the expression of one of several DNA damage response proteins (e.g., 53PBP1), it is a more versatile index of telomere dysfunction. Indeed, the TIF assay should distinguish between senescence in response to telomere shortening (replicative senescence) or senescence due to culture conditions (stasis or culture shock) (reviewed in [3, 32]). Detection of TIFs in tissues of donors suspected of telomere abnormalities (such as dyskeratosis congenita, RecQ helicase syndromes, and aging) (reviewed in [1, 33]) might reveal instances of telomere dysfunction in vivo. Additionally, TIFs will be a valuable indicator of telomere status in cells deficient for telomere-protective factors that have no overt telomere fusion phenotype. Finally, TIFs could reveal telomere dysfunction during various steps of human tumorigenesis. Demonstration of uncapped telomeres in human cancer may allow for direct testing of the proposal that telomere dysfunction drives genome instability during tumorigenesis (reviewed in [2, 34]).

The DNA damage response in mammalian cells has been studied by using a variety of nonphysiological treatments, including ionizing radiation, radiomimetic drugs, UV light, and laser treatment. Acute telomere uncapping with TRF2 is yet another means of inducing DNA damage. The advantage of this method is that the site of the lesion can be easily recognized by using telomeric markers and that the exact DNA structure of uncapped telomeres can be determined.

Experimental Procedures

Cell strains, cell culture procedures, viral gene delivery, immunoblotting, and IF techniques have been described previously [6, 13, 14, 35, 36]. Experimental details and sources of antibodies are given in the Supplemental Data available with this article online.

For TRF2 RNAi, double-stranded siRNA were designed to target

nt 402–422 (#2) or nt 1466–1484 (#4) of the human TRF2 cDNA (NM-005652) according to published methods [37]. HeLa1.2.11 or HeLaII cells were transfected by using Oligofectamine (Invitrogen) according to the manufacturer's instructions. Briefly, 2.1×10^5 cells per well in a 6-well plate were plated 18–24 hr prior to transfection. Transfections were done twice with a 24-hr interval. Cells were processed 40–96 hr after the first transfection. As a control, an siRNA designed to target GFP was used.

Supplemental Data

Supplemental Data including detailed Experimental Procedures are available at http://www.current-biology.com/cgi/content/full/13/17/1549/DC1.

Acknowledgments

We thank Thanos Halazonetis, Mike Kastan, and Chris Bakkenist for antibodies. John Petrini is thanked for comments on this manuscript. Jan Karlseder, Richard Wang, Diego Loayza, and Josh Silverman are thanked for technical advice. We are grateful to Mr. Frank Pearl and Dr. Alison North for providing us with the opportunity to use the DeltaVision microscope. Members of the de Lange lab are thanked for discussion of this project. This work was supported by grants from the National Institutes of Health (NIH) to T.d.L. (GM49046 and AG16643). H.T. is supported by a Charles H. Revson fellowship. A.S. was supported by an NIH MSTP grant (GM07739) to the Cornell/RU/MSK Tri-Institutional MD/PhD program.

Received: May 23, 2003
Revised: July 8, 2003
Accepted: July 16, 2003
Published online: July 23, 2003

References

1. Marciniak, R.A., Johnson, F.B., and Guarente, L. (2000). Dyskeratosis congenita, telomeres and human ageing. Trends Genet. *16*, 193–195.
2. Maser, R.S., and DePinho, R.A. (2002). Connecting chromosomes, crisis, and cancer. Science *297*, 565–569.
3. Campisi, J. (2001). Cellular senescence as a tumor-suppressor mechanism. Trends Cell Biol. *11*, S27–S31.
4. Campisi, J., Kim, S.H., Lim, C.S., and Rubio, M. (2001). Cellular senescence, cancer and aging: the telomere connection. Exp. Gerontol. *36*, 1619–1637.
5. de Lange, T. (2002). Protection of mammalian telomeres. Oncogene *21*, 532–540.
6. Karlseder, J., Broccoli, D., Dai, Y., Hardy, S., and de Lange, T. (1999). p53- and ATM-dependent apoptosis induced by telomeres lacking TRF2. Science *283*, 1321–1325.
7. Vaziri, H., and Benchimol, S. (1996). From telomere loss to p53 induction and activation of a DNA-damage pathway at senescence: the telomere loss/DNA damage model of cell aging. Exp. Gerontol. *31*, 295–301.
8. Shay, J.W., Wright, W.E., Brasiskyte, D., and Van der Haegen, B.A. (1993). E6 of human papillomavirus type 16 can overcome the M1 stage of immortalization in human mammary epithelial cells but not in human fibroblasts. Oncogene *8*, 1407–1413.
9. Chin, L., Artandi, S.E., Shen, Q., Tam, A., Lee, S.L., Gottlieb, G.J., Greider, C.W., and DePinho, R.A. (1999). p53 deficiency rescues the adverse effects of telomere loss and cooperates with telomere dysfunction to accelerate carcinogenesis. Cell *97*, 527–538.
10. Broccoli, D., Smogorzewska, A., Chong, L., and de Lange, T. (1997). Human telomeres contain two distinct Myb-related proteins, TRF1 and TRF2. Nat. Genet. *17*, 231–235.
11. Bilaud, T., Brun, C., Ancelin, K., Koering, C.E., Laroche, T., and Gilson, E. (1997). Telomeric localization of TRF2, a novel human telobox protein. Nat. Genet. *17*, 236–239.
12. van Steensel, B., Smogorzewska, A., and de Lange, T. (1998). TRF2 protects human telomeres from end-to-end fusions. Cell *92*, 401–413.
13. Smogorzewska, A., Karlseder, J., Holtgreve-Grez, H., Jauch, A., and de Lange, T. (2002). DNA Ligase IV-Dependent NHEJ of Deprotected Mammalian Telomeres in G1 and G2. Curr. Biol. *12*, 1635–1644.
14. Smogorzewska, A., and de Lange, T. (2002). Different telomere damage signaling pathways in human and mouse cells. EMBO J. *21*, 4338–4348.
15. Bakkenist, C.J., and Kastan, M.B. (2003). DNA damage activates ATM through intermolecular autophosphorylation and dimer dissociation. Nature *421*, 499–506.
16. Bao, S., Tibbetts, R.S., Brumbaugh, K.M., Fang, Y., Richardson, D.A., Ali, A., Chen, S.M., Abraham, R.T., and Wang, X.F. (2001). ATR/ATM-mediated phosphorylation of human Rad17 is required for genotoxic stress responses. Nature *411*, 969–974.
17. Mirzoeva, O.K., and Petrini, J.H. (2001). DNA damage-dependent nuclear dynamics of the Mre11 complex. Mol. Cell. Biol. *21*, 281–288.
18. Nelms, B.E., Maser, R.S., MacKay, J.F., Lagally, M.G., and Petrini, J.H. (1998). In situ visualization of DNA double-strand break repair in human fibroblasts. Science *280*, 590–592.
19. Paull, T.T., Rogakou, E.P., Yamazaki, V., Kirchgessner, C.U., Gellert, M., and Bonner, W.M. (2000). A critical role for histone H2AX in recruitment of repair factors to nuclear foci after DNA damage. Curr. Biol. *10*, 886–895.
20. Schultz, L.B., Chehab, N.H., Malikzay, A., and Halazonetis, T.D. (2000). p53 binding protein 1 (53BP1) is an early participant in the cellular response to DNA double-strand breaks. J. Cell Biol. *151*, 1381–1390.
21. DiTullio, R.A., Jr., Mochan, T.A., Venere, M., Bartkova, J., Sehested, M., Bartek, J., and Halazonetis, T.D. (2002). 53BP1 functions in an ATM-dependent checkpoint pathway that is constitutively activated in human cancer. Nat. Cell Biol. *4*, 998–1002.
22. Zhu, X.D., Kuster, B., Mann, M., Petrini, J.H., and Lange, T. (2000). Cell-cycle-regulated association of RAD50/MRE11/NBS1 with TRF2 and human telomeres. Nat. Genet. *25*, 347–352.
23. Rogakou, E.P., Boon, C., Redon, C., and Bonner, W.M. (1999). Megabase chromatin domains involved in DNA double-strand breaks in vivo. J. Cell Biol. *146*, 905–916.
24. Shiloh, Y. (2001). ATM and ATR: networking cellular responses to DNA damage. Curr. Opin. Genet. Dev. *11*, 71–77.
25. Mirzoeva, O.K., and Petrini, J.H.J. (2003). DNA replication-dependent nuclear dynamics of the Mre11 complex. Mol. Cancer Res. *1*, 207–218.
26. Wood, L.D., Halvorsen, T.L., Dhar, S., Baur, J.A., Pandita, R.K., Wright, W.E., Hande, M.P., Calaf, G., Hei, T.K., Levine, F., et al. (2001). Characterization of ataxia telangiectasia fibroblasts with extended life-span through telomerase expression. Oncogene *20*, 278–288.
27. Nakamura, H., Fukami, H., Hayashi, Y., Kiyono, T., Nakatsugawa, S., Hamaguchi, M., and Ishizaki, K. (2002). Establishment of immortal normal and ataxia telangiectasia fibroblast cell lines by introduction of the hTERT gene. J. Radiat. Res. (Tokyo) *43*, 167–174.
28. Zou, L., and Elledge, S.J. (2003). Sensing DNA damage through ATRIP recognition of RPA-ssDNA complexes. Science *300*, 1542–1548.
29. Stewart, S.A., Ben-Porath, I., Carey, V.J., O'Connor, B.F., Hahn, W.C., and Weinberg, R.A. (2003). Erosion of the telomeric single-strand overhang at replicative senescence. Nat. Genet. *33*, 492–496.
30. Garvik, B., Carson, M., and Hartwell, L. (1995). Single-stranded DNA arising at telomeres in cdc13 mutants may constitute a specific signal for the RAD9 checkpoint. Mol. Cell. Biol. *15*, 6128–6138.
31. Gardner, R., Putnam, C.W., and Weinert, T. (1999). RAD53, DUN1 and PDS1 define two parallel G2/M checkpoint pathways in budding yeast. EMBO J. *18*, 3173–3185.
32. Sherr, C.J., and DePinho, R.A. (2000). Cellular senescence: mitotic clock or culture shock? Cell *102*, 407–410.
33. Hickson, I.D. (2003). RecQ helicases: caretakers of the genome. Nat. Rev. Cancer *3*, 169–178.
34. de Lange, T. (1995). Telomere dynamics and genome instability in human cancer. In Telomeres, E.H.B.a.C.W. Greider, ed. (CSH: CSH press), pp. 265–293.

35. Karlseder, J., Smogorzewska, A., and de Lange, T. (2002). Senescence induced by altered telomere state, not telomere loss. Science *295*, 2446–2449.
36. Smogorzewska, A., van Steensel, B., Bianchi, A., Oelmann, S., Schaefer, M.R., Schnapp, G., and de Lange, T. (2000). Control of human telomere length by TRF1 and TRF2. Mol. Cell. Biol. *20*, 1659–1668.
37. Elbashir, S.M., Harborth, J., Lendeckel, W., Yalcin, A., Weber, K., and Tuschl, T. (2001). Duplexes of 21-nucleotide RNAs mediate RNA interference in cultured mammalian cells. Nature *411*, 494–498.

Supplemental Data

DNA Damage Foci at Dysfunctional Telomeres

Hiroyuki Takai, Agata Smogorzewska, and Titia de Lange

Supplemental Experimental Procedures

Analysis of Cells with Inhibited TRF2 Function

Cell strains, cell culture procedures, and viral gene delivery have been described previously [S1–S4]. Adenovirus was used at 100 pfu/cell for IMR90 and at 400 pfu/cell for hTERT-BJ and A-T cells, unless otherwise indicated. Indirect immunofluorescence procedures were performed as described [S5]. The following antibodies were used: TRF1, 371 [S6] or mouse anti-hTRF1 serum (unpublished data); TRF2, 647 [S7]; 53BP1 Mab (generously provided by T. Halazonetis); Mre11, 874 [S7]; ATM 1981S-P ([S8]; generously provided by M. Kastan); γ-H2AX, JBW301 (Upstate); Rad17 Ser 645, #3421 (Cell Signaling); PCNA, PC10 (BD Biosciences); Phospho-H3, 6G3 (Cell Signaling). The TIF index was determined on TRF1/53BP1 dual IF by capturing images of at least 5 randomly chosen fields with 5–10 nuclei each. For PCNA staining, an in situ cell fractionation procedure was performed [S9]. The antibodies used for Western blotting were as described [S3]; p16 was detected with C-20 (Santa Cruz). Western blotting for ATM was done by using sonicated lysates of 20 million cells per milliliter in buffer containing 50 mM Tris-HCl (pH 7.5), 150 mM NaCl, 10% v/v glycerol, 1% v/v Tween 20, 50 mM Na-β-glycerophophate, 1 mM NaF, 1 mM $NaVO_4$, 0.1 mM DTT, 0.5 mM PMSF, 0.5 μg/ml leupeptin. Proteins were blotted onto PVDF membrane (Milllipore) and were probed with 2C1 (GeneTex). The SA-β-gal assay [S10] was performed 2 days after seeding 1×10^5 cells per well in a 6-well plate at the indicated time points after selection [S11]. BrdU incorporation experiments were executed as described in [S3]. Micrographs were recorded on a Zeiss Axioplan II microscope with a Hamamatsu C4742-95 digital camera by using the Improvision Open Lab program. The images were corrected for background and were merged with Adobe Photoshop. For Figures 1A and 2, six serial images were taken every 0.2 μm and were integrated to one image by using the Open Lab program. For Figure 1B, images were captured as three-dimensional volumes by using a DeltaVision Imaging Restoration Microscope (Applied Precision Instruments) on an Olympus IX-70 microscope. The images were subsequently deconvolved by using iterative constrained deconvolution.

Supplemental References

S1. Karlseder, J., Broccoli, D., Dai, Y., Hardy, S., and de Lange, T. (1999). p53- and ATM-dependent apoptosis induced by telomeres lacking TRF2. Science *283*, 1321–1325.

S2. Smogorzewska, A., Karlseder, J., Holtgreve-Grez, H., Jauch, A., and de Lange, T. (2002). DNA Ligase IV-dependent NHEJ of deprotected mammalian telomeres in G1 and G2. Curr. Biol. *12*, 1635–1644.

S3. Smogorzewska, A., and de Lange, T. (2002). Different telomere damage signaling pathways in human and mouse cells. EMBO J. *21*, 4338–4348.

S4. Karlseder, J., Smogorzewska, A., and de Lange, T. (2002). Senescence induced by altered telomere state, not telomere loss. Science *295*, 2446–2449.

S5. Smogorzewska, A., van Steensel, B., Bianchi, A., Oelmann, S., Schaefer, M.R., Schnapp, G., and de Lange, T. (2000). Control of human telomere length by TRF1 and TRF2. Mol. Cell. Biol. *20*, 1659–1668.

S6. van Steensel, B., and de Lange, T. (1997). Control of telomere length by the human telomeric protein TRF1. Nature *385*, 740–743.

S7. Zhu, X.D., Kuster, B., Mann, M., Petrini, J.H., and Lange, T. (2000). Cell-cycle-regulated association of RAD50/MRE11/NBS1 with TRF2 and human telomeres. Nat. Genet. *25*, 347–352.

S8. Bakkenist, C.J., and Kastan, M.B. (2003). DNA damage activates ATM through intermolecular autophosphorylation and dimer dissociation. Nature *421*, 499–506.

S9. Mirzoeva, O.K., and Petrini, J.H. (2001). DNA damage-dependent nuclear dynamics of the Mre11 complex. Mol. Cell. Biol. *21*, 281–288.

S10. Dimri, G.P., Lee, X., Basile, G., Acosta, M., Scott, G., Roskelley, C., Medrano, E.E., Linskens, M., Rubelj, I., Pereira-Smith, O., et al. (1995). A biomarker that identifies senescent human cells in culture and in aging skin in vivo. Proc. Natl. Acad. Sci. USA *92*, 9363–9367.

S11. van Steensel, B., Smogorzewska, A., and de Lange, T. (1998). TRF2 protects human telomeres from end-to-end fusions. Cell *92*, 401–413.